JOURNAL OF MATERIALS SCIENCE 15 (1980) 765–772

New aspects of the microhardness of ultraoriented polyethylene

F. J. BALTÁ-CALLEJA, D. R. RUEDA
Instituto de Estructura de la Materia, CSIC, Madrid 6, Spain

R. S. PORTER, W. T. MEAD
Polymer Science and Engineering Department, Materials Research Laboratory, University of Massachusetts, Amherst, Massachusetts 01003, USA

The influence of extrusion conditions on the microhardness of ultradrawn polyethylene (PE) has been investigated. The micromechanical behaviour of ultradrawn PE fibres can be defined in terms of a creep constant and a microhardness value (*MH*) at 0.1 min, relating to the size of indentation under load rather than to the residual dimension. The PE strands show, in addition, a conspicuous anisotropic shape of the indentation pattern ($MH_{\parallel} > MH_{\perp}$) which involves a local elastic recovery of the material parallel to the fibre axis. The hardening of the fibres in the parallel and perpendicular direction to the fibre axis is an increasing function of both extrusion temperature and extrusion pressure and can be explained in terms of a simultaneous improvement in the strength and the lateral packing of fibrils and microfibrils in fibre direction. For extrusion temperatures (T_e) greater than 134° C the microhardness shows, however, a decrease which is thought to be related to the molecular relaxation occurring in the vicinity of the melting point. In the range of extrusion temperatures (90 to 137° C) and extrusion pressures (0.24 to 0.5 GPa) investigated, the hardness anisotropy on the fibre surface, ΔMH, is a unique increasing function of draw ratio λ. It is completely independent of both the extrusion temperature and pressure. ΔMH in the core of cleaved fibres shows a constant value which is independent of λ and equals the extrapolated value at the surface for the maximum attainable value of λ. The results can be satisfactorily explained if one considers the existing morphological differences between the outer sheath and the inner core of the fibres.

1. Introduction

In previous investigations [1–3] we have shown that microhardness indentation (*MH*) can be a very useful method, indeed, for the investigation of the anisotropy and microstructure of oriented semicrystalline polymers. The discontinuous variation of *MH* along the neck (i.e. *MH* versus λ) of plastically deformed PE parallels, for instance [1], the abrupt transformation from the original microspherulitic into the fibre structure according to the model of plastic deformation proposed by Peterlin [4]. Furthermore, the increase of *MH* parallel to the deformation direction with draw ratio can be correlated to the increasing number of tie molecules in the fibrous structure [1]. In the case of hydrostatically-annealed (at 5.3 kbar) oriented PE [2], the *MH* is an increasing function of annealing temperature and consequently of chain extension. Further, the Vickers *MH* test has been utilized as an additional tool for the determination of the microstructure of injection moulded semicrystalline thermoplastics. Bowmann and Bevis [5] have proved in this case that the *MH* test clearly describes the extent of the different structures and the degree of the preferred chain axis orientation within each structure. A further illustration of the value of this technique is the recent investigation of Nakayama and Kanetsuna [6] on the simultaneous study of *MH* and other structural parameters, as a result of plastic defor-

0022–2461/80/030765–8$02.80/0

mation of high density PE during hydrostatic extrusion. Here the microhardness of extruded PE increased with increasing extrusion ratio.

Perhaps, the most salient feature of all deformed and/or extruded PE samples is the clear anisotropy exhibited by the indentation pattern. The anisotropy of the *MH*, similar to other mechanical properties, is a consequence of the high orientation of polymer chains in both crystalline and non-crystalline regions. For uniaxially anisotropic polymers there appear varying hardness values which lie between the *MH* parallel and perpendicular to the chain direction [2]. In oriented polymers a certain amount of elastic recovery occurs on unloading, so that the indentation contracts anisotropically. However, as far as we know, no corrections for instant elastic recovery in oriented systems have been reported. Since the indentation process at the surface of the oriented polymer is, however, primarily controlled by irreversible deformation under the indenter the *MH* is expected to be directly correlated to the specific modes of plastic deformation in semi-crystalline polymers. These will be predominantly determined by the structure and packing of the building units – in our case fibrils, microfibrils, stacks of crystalline lamellas – and their connection by tie molecules in the axial direction of the fibrous material and may involve bending and slippage of fibrils, crack formation, chain tilt and slip and chain unfolding as well as other mechanisms.

The present study will be confined to *MH* measurements performed on ultra-oriented PE fibres prepared by solid state extrusion using an Instron capillary Rheometer [7, 8]. This process has been developed to achieve polymers of high tensile moduli and is based on reaching co-operative continuity for oriented high-strength covalent bonds of a multitude of parallel polymer chains [9]. The extended high density PE filaments show unusually high crystal orientation [10] ($\sim 0.996 \pm 0.002$), chain extension, axial modulus (67 GPa) and ultimate tensile strength (0.48 GPa) [11]. The present contribution complements a previous study [3] on *MH* of ultra-oriented PE and extends the *MH* experiments to samples isothermally crystallized within a wider range of extrusion temperatures, T_e, and two different extrusion pressures, P_e. Firstly, we shall recapitulate the salient features of the indentation process; secondly, we shall discuss the relationship between hardness and extrusion conditions with special emphasis on mechanical anisotropy; and thirdly, we shall compare the experimentally determined values with the calculations based on an assessment of intermolecular forces.

1.1. The indentation process

Hardness is a basic property – it represents resistance to deformation at the polymer surface – since there is a close relationship between hardness and yield stress in the ideal case (stress at the local maximum of the true stress–strain curve). The indentation test provides the most general method for the measurement of hardness and its mechanism has been defined by Tabor [12]. Pyramid indentors are best suited for the test: firstly, because they provide a contact pressure which is independent of indent size; and secondly, because they are less affected by elastic release than other indenters. The hardness can be visualized by the momentary reaction which the polymer surface exerts during a small amount of yielding or plastic straining as by compression. This reaction, which in the case of a sharp indenter is highly localized to a small volume element, involves elastic and viscous effects and eventually a certain friction. When the pyramid starts pressing onto the polymer surface the material first deforms elastically. After the stresses exceed the elastic limit, plastic flow through various possible molecular mechanisms occurs. The material beneath the indenter becomes permanently displaced and a microimpression arises. The *MH*, which is directly proportional to the pressure beneath the indenter, can then be evaluated after load removal by observing the length of the diagonals of indentation, after allowing for elastic release.

In the present paper we wish also to report on the time dependence of indentation during loading. The tendency of polymers to creep under a constant stress involves a time factor in the indentation experiment [13, 14]. Here is involved a viscosity element and the question arises as to whether one must wait until the indentation comes to an equilibrium before the hardness measurement is made. Whether the material is relatively hard or soft depends upon the time for which the indentation stress is applied. This aspect of the problem is called creep and is closely connected with the rheological properties of the material. Thus, contrary to hard metals, polymers do flow under indentation at room temperature and equilibrium

if ever obtained may eventually require several weeks or months.

2. Experimental procedure

2.1. Materials and extrusion details

The fibres were prepared by the method reported by Porter *et al.* [15]. Alathon 7050 (Dupont, $M_w = 5.9 \times 10^4$) high density PE was used in this study. According to this method, strong ultra-oriented strands of high density PE, free from defects and of great length, were extruded in an Instron Capillary Rheometer. Pressure, temperature and capillary geometry are the most important parameters in the preparation of ultra-oriented fibres. The polymer was isothermally (134° C) and hydrostatically (0.24 GPa) crystallized. Thereafter, it was allowed to cool or warm at ~ 1° C min^{-1} to the desired extrusion temperature, while maintaining the pressure. A $2\theta = 20°$ included-angle, conical, stainless steel die was used with a maximum draw ratio equal to 51. The quoted draw ratios are defined as the ratio of the cross-sectional area of the entrance of the conical die of radius R_m and the exit of the die of radius R_b. The actual draw ratio may be directly calculated from the following expression

$$\lambda = \left(1 + \frac{3L \tan \theta}{R_b}\right)^{2/3}, \quad (1)$$

where L is the length of the fibre extruded, θ the semi-angle of die, and R_b the radius of the die at the exit of the cone and equal to the radius of the fibre assuming no extrudate expansion. For the fibres investigated $R_b = 0.0685$ cm. In order to calculate the draw ratio at a particular point one has thus simply to measure the length from the leading edge – at a draw ratio of unity (opaque). At the other end – the highest draw ratio – a fracture phenomenon associated with deformation of highly anisotropic PE occurs. It is important to mention that, as the extrusion temperature is lowered, fracture occurs at lower draw ratios. Hence, we could not cover the complete draw ratio range from the various temperatures investigated. Table I shows the temperatures and applied pressures of extrusion used in these experiments.

TABLE I Extrusion conditions of the ultra-oriented high density polyethylene fibres crystallized at 134° C under 0.24 GPa

Sample	Extrusion temperature (° C)	Extrusion pressure (GPa)
1	90	0.24
2	120	0.24
3	134	0.24
4	137	0.24
5	120	0.50

2.2. Microhardness measurements

The *MH* measurements were carried out at room temperature with a Leitz hardness apparatus using a Vickers square pyramidal diamond. A micrometer eyepiece of the microscope permitted the measurement of the indentations to be made within ± 0.5 μm. The distance between the diamond tip and surface is 40 μm. The load was applied for a time $\tau = t_t + t$ where $t_t \sim 8$ sec is the sinking time of the diamond until the surface is reached and t is the actual loading time. Values of t of 0.1, 0.5, 1.0, 3, 6, 10 and 20 min were selected. A series of at least 10 indentations for the first two times, 5 indentations for the following three and two indentations for the last two times were made for each sample. The final permanent deformation was instantly measured after load release so that long delayed recovery would be negligible. The instant elastic recovery of the indentation d_o, in μm, was derived from the intercept $P_0 = d_o^2 \tan \alpha$ of the plot P versus d^2 (where $\tan \alpha$ is the slope of the plot and d is the length of the indentation diagonal). Ten measurements at 0.1 min were respectively made with $P = 15$ g and $P = 100$ g for each sample. The hardness value was calculated from the projected area of the indentation allowing for the correction due to instant elastic recovery according to

$$MH = k \frac{P}{(d + d_o)^2} \text{ (GPa)}, \quad (2)$$

where P is the load in kg and d and d_o are the respective plastic and elastic contributions to indentation in μm and k is a constant equal to 18 180.

3. Results

3.1. Elastic release

Fig. 1 illustrates the increase for sample 2 of the uncorrected, $MH_{\parallel}^*, MH_{\perp}^*$ (i.e. assuming $d_o = 0$ in Equation 2) and corrected values of *MH* for instant elastic recovery as a function of λ for a time $t \sim 0.1$ min. These data show that this correction is quite noticeable in the fibre direction ($P_0 \sim 0.1$ to 0.4 g) contributing to an elastic release of approximately up to 20% in all samples

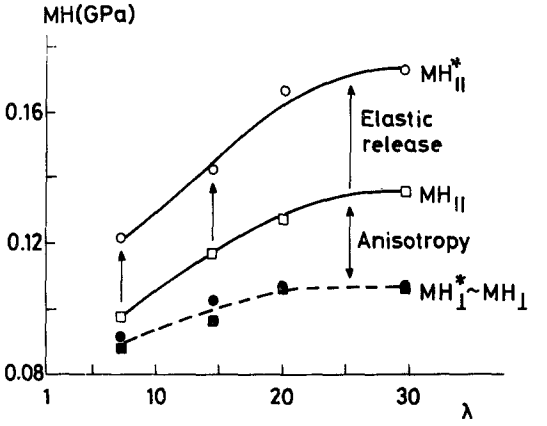

Figure 1 Vickers microhardness, MH, of an ultra-oriented PE strand (sample no. 2, Table I) as a function of draw ratio, λ. $P = 0.015$ kg, $t = 0.1$ min. On unloading the material suffers an elastic release and the $MH_{\parallel}$ value underload is transformed into the apparent one $MH^*_{\parallel}$. The hardness anisotropy of the fibres is defined as $\Delta MH = MH_{\parallel} - MH_{\perp}(\%)$. In the direction perpendicular to the fibre axis there is no elastic release.

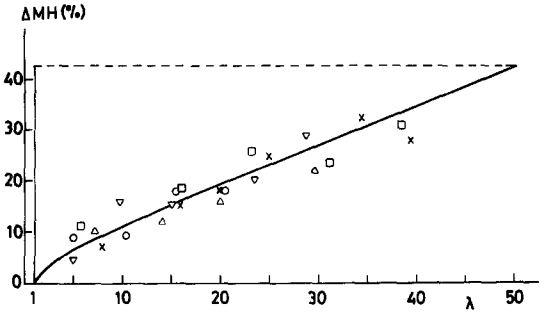

Figure 2 Microhardness anisotropy, $\Delta MH = MH_{\parallel} - MH_{\perp}$ (%) in the inner core (dotted line) and on the surface of ultra-oriented PE extruded at 0.24 GPa: ○, 90° C; △, 120° C; □, 134° C; ▽ 137° C and X, 0.5 GPa, 120° C. The tests were performed at $P = 0.015$ kg ($P = 0.05$ kg in the core) and $t = 0.1$ min. The continuous curve follows the expression: $\Delta MH = a(\lambda - 1)^b$; where $a = 1.42$ and $b = 0.86$.

investigated. The instant elastic release is, however, negligible in the direction perpendicular to the fibre axis ($P_0 \sim 0$ and hence $d_o \sim 0$). The same trend is obtained for the rest of the samples in Table I.

3.2. Microhardness anisotropy

The most relevant feature of these highly oriented PE samples is the conspicous anisotropy shown by the indentation pattern. The Vickers hardness is maximum when the indentation diagonal is parallel to the fibre axis, $MH_{\parallel}$, and minimum when normal to it, $MH_{\perp}$. In addition both $MH_{\parallel}$ and $MH_{\perp}$ are a function of draw ratio, λ, as shown in Fig. 1. The measurement of microhardness anisotropy $\Delta MH = MH_{\parallel} - MH_{\perp}(\%)$ in these fibres substantiates our previous results [3] and offers a wider and more complete set of data. Fig. 2, thus shows the clear increase of ΔMH with λ according to a power law

$$\Delta MH = a(\lambda - 1)^b. \qquad (3)$$

The least-square fit offers a correlationn coefficient 0.91 and a and b are fitting constants equal to 1.42 and 0.86 respectively. Equation 3 yields a limiting value for $\lambda_{max} = 51$ of $\Delta MH \sim 42\%$. This is the highest possible anisotropy of strands which can be obtained for the capillary entrance angle of 20° used.

3.3. Loading time dependence: creep constant

The final size of indentation is a function of time underload. Most revealing is the log–log plot of MH versus t. Fig. 3 illustrates this plot for the sample No. 2 at three different draw ratios. The data yield straight lines with a correlation coefficient better than 0.98. Both $MH_{\parallel}$ and $MH_{\perp}$ values clearly increase with λ. Microindentation hardness can be written, hence, as

$$MH = MH_{0.1}\, t^{-K}, \qquad (4)$$

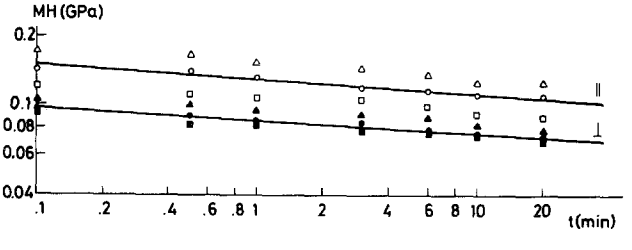

Figure 3 Log–log plot illustrating the loading time dependence of $MH_{\parallel}$ and $MH_{\perp}$ for three draw ratio values in sample 2 ($P = 0.015$ kg). The plot yields a law $MH = MH_{0.1}\, t^{-K}$ where K is the creep constant and $MH_{0.1}$ the hardness for $t = 0.1$ min [λ = 7(□); 15(○); 29(△)].

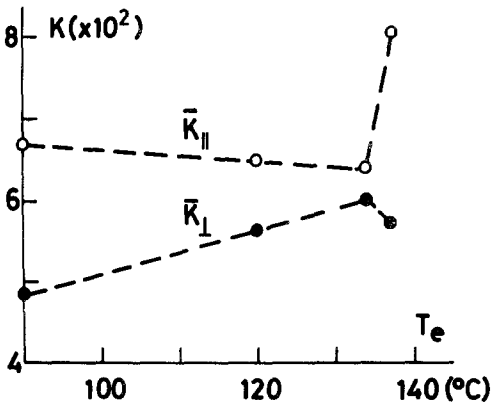

Figure 4 The creep constant K in the direction parallel and perpendicular to the fibre axis of ultra-oriented PE as a function of extrusion temperature.

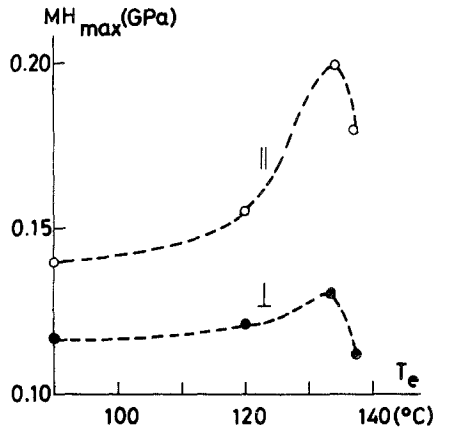

Figure 6 Extrapolated microhardness values for $\lambda_{max} = 51$, parallel and perpendicular to the fibre axis as a function of extrusion temperature $P = 0.015$ kg, $t = 0.1$ min., Extrusion pressure = 0.24 GPa.

where $MH_{0.1}$ is the hardness value at $t = 0.1$ min and K is the slope of the plot. The constant K provides a quantitative measure of the rate of creep of the material under the indenter. The analysis of data reveals that K is also an anisotropic quantity, $K_{\parallel} > K_{\perp}$, independent of λ. Fig. 4 illustrates the average values of $\bar{K}_{\parallel}$ and $\bar{K}_{\perp}$ as a function of extrusion temperature. Thus $\bar{K}_{\parallel}$ gradually decreases whereas $\bar{K}_{\perp}$ increases with T_e up to $T_e = 134°$ C. At $T_e = 137°$ C $\bar{K}_{\parallel}$ suffers a sudden increase while $\bar{K}_{\perp}$ decreases.

3.4. Influence of the temperature and pressure of extrusion

The corrected values of microhardness at $t = 0.1$ parallel and perpendicular to the fibre axis are plotted in Fig. 5 as a function of λ for various extrusion temperatures. The maximum λ values given are situated in the vicinity of the fracture end for each fibre. For extrusion temperature of 90 and 120° C, both, $MH_{\parallel}$ and $MH_{\perp}$ show a gradual increase (according to a power curve), levelling off for $\lambda > 30$. The increase of $MH_{\parallel}$, and $MH_{\perp}$, with λ becomes more conspicous (turning into an exponential character) at the higher extrusion temperatures of 134° C and 137° C respectively. If one attempts an extrapolation of MH for the maximum value of $\lambda_{max} = 51$, for the 20° conical angle used, one can then inspect the variation of the limiting values of $MH_{\parallel}$ and $MH_{\perp}$ with the temperature of extrusion. Fig. 6 illus-

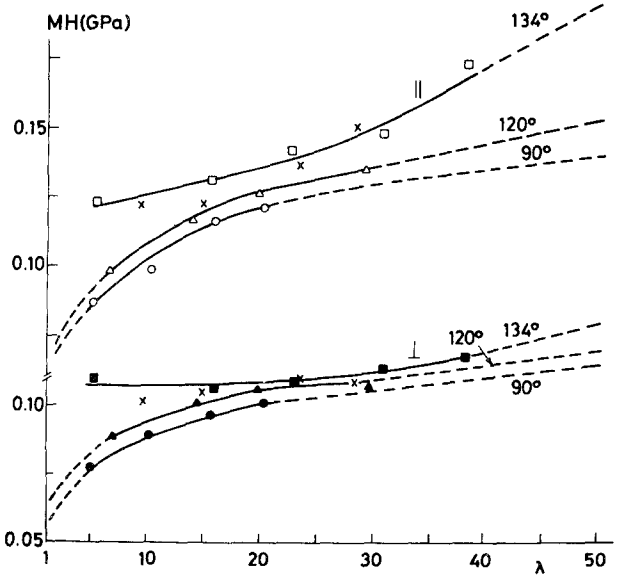

Figure 5 Vickers microhardness in the direction (a) parallel and (b) perpendicular to the fibre axis of ultra-oriented PE as a function of draw ratio for various extrusion temperatures as indicated. The crosses correspond to a temperature of 137° C, $P = 0.015$ kg, $t = 0.1$ min. Extrusion pressure = 0.24 GPa.

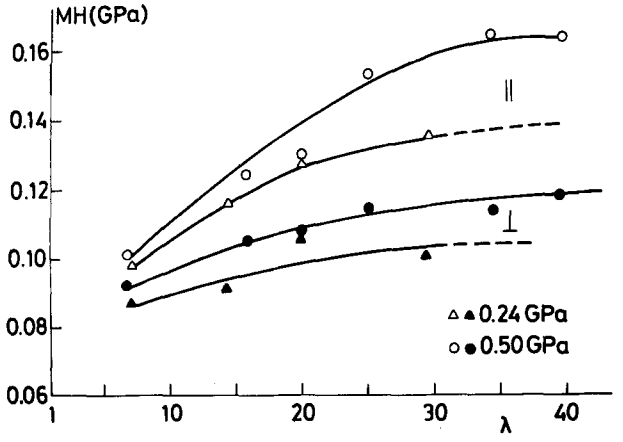

Figure 7 Vickers microhardness, parallel and perpendicular to the fibre axis of ultra-oriented PE as a function of draw ratio for two extrusion pressures $P = 0.015$ kg, $t = 0.1$ min., Extrusion temperature: 120° C.

trates the marked increase of $MH_{\max\parallel}$ with T_e up to 134° C and then a decrease above 134° C. The increase of $MH_{\max\perp}$ is less conspicous but also shows a reduction above 134° C.

The clear effect of extrusion pressure on hardness while maintaining the extrusion temperature constant is illustrated in Fig. 7. The mechanical properties are evidently improved with extrusion pressure. An increase of about 20% (12%) in $MH_{\parallel}$ ($MH_{\perp}$) for $\lambda \sim 30$ is for example obtained when the extrusion pressure is doubled.

4. Discussion

The above results (Figs. 5 to 7) reveal a hardening of PE, through the simultaneous influence of flow extrusion drawing and high pressure realized in the Instron Capillary Rheometer. It is known that uniaxial plastic deformation induces drastic changes in the orientation of molecular chains and transforms the initial microspherulitic structure into an anisotropic fibre structure [16, 17]. The resulting highly oriented fibrous texture consists of highly aligned fibrils (~ 300 nm) and microfibrils 10–20 nm in lateral dimensions in which stacks of crystal blocks perpendicularly oriented to the fibre direction (*c*-axis) act as cross links for the tie molecules bridging adjacent crystals [18]. Previous studies have shown that a fraction of fibrils (~ 10% to 15%) are composed of extended chain crystals [9]. The crystalline chains, the microfibrils and the total strand possess the same high alignment. Radial strength is thus limited to weak van der Waals forces. Accordingly, the strands show a very easy cleavage and crush when compressed along the radius axis.

Although the Vickers indenter imposes nearly a spherically symmetrical strain* on the sample surface, the strain field developed beneath is asymmetrical because the material is highly anisotropic. The stresses are obviously larger along the fibre axis because the material is stiffest in this direction. Thus, since the indentation is symmetric while the load is applied, the altered shape of the final impression must arise on unloading. The observed anisotropy of the plastic impression is, hence, admittedly due to an elastic recovery of the strands in fibre direction. There is very little doubt that $MH_{\parallel}$ which represents the main contribution to the increasing ΔMH value will depend, to some extent on the longitudinal elastic modulus, $E_{\parallel}$. The concurrent increase of $E_{\parallel}$ and λ in drawn PE [22] supports in fact the assumption that tie molecules interconnecting the stacked lamellas are the main contributor to the longitudinal mechanical strength of fibres. The indentation mechanism undergone by these fibres involves, in addition, a rather complex combination of various contributions. These include: (a) an elastic release; (b) a partial plastic deformation; and (c) a creep effect.

A true elastic release below the indenter (proportional to P_0) only occurs parallel to the fibre direction and is negligible at right angles to it. This constant true elastic release (to be differentiated from the anisotropic elastic recovery (see Fig. 1) is of the order of -20% for the investigated samples and is nearly independent of λ. Equation 2 provides for the correction to this elastic effect allowing for the evaluation of the true plastic contribution to indentation parallel and perpen-

* Several authors [19–21] have approximated the problem of penetration by an indenter to that of the expansion of a spherical cavity in an infinite plastic–elastic medium.

dicular to the fibre axis. After exceeding the initial yield stress the strands deform at a constant rate indicating that a viscous type of flow under compressive load is taking place. Similarly to the case of isotropic PE [23] an expression for the hardness of ultra-oriented PE, $MH = MH_{0.1}\, t^{-K}$, that responds to a constant rate creep process is found. $MH_{0.1}$, the hardness at 0.1 min (i.e. when $\log t \to 0$) is a quantity directly proportional to the yield stress of the material. According to the classical plasticity theory [12] $MH \sim 3Y$ (Tabor's relation). This is, indeed, an interesting expression which correlates the microscopic local behaviour of the fibrils with the bulk mechanical properties of the strand. Previous results [23] obtained on isotropic PE samples indicate that the hardness value at 0.1 min approaches, depending on morphology, the value predicted by Tabor's relation. The constant K represents the constant rate at which the material creeps under the indenter yielding the observed decrease in hardness.

The microhardness is strongly affected by the extrusion conditions of these fibres. This has been previously pointed out by Nakayama and Kanetsuna [6]. These authors report only the hardness value parallel to the extrusion direction. Hence, no information on anisotropy is provided. Neither data on elastic release nor on creep effects are given by these authors. The hardening of our ultra-oriented PE with extrusion temperature (Fig. 6) parallels the increase in stiffness measured previously [9]. This double increase originates from a combination of increased strength in fibre direction and improvement in the lateral microfibril packing offering as a result a higher resistance to plastic deformation in the radial direction. The rate of creep $\bar{K}_{\|}$ in fibre direction concurrently decreases with T_e (Fig. 4) pointing to an improvement of individual fibril properties – crystalline weight fraction and crystalline orientation increase. The creep, $\bar{K}_{\perp}$, normal to the fibre direction simultaneously increases, however, suggesting the development of microfibrillarity at higher extrusion temperatures. Above 134° C relaxation and partial melting of fibrils occurs at the capillary exit. This results in a decrease of the hardness value (Fig. 6) and a simultaneous sudden increase and decrease of the creep constant in the parallel and perpendicular direction to the fibre axis (Fig. 4) respectively.

Extrusion at higher pressure also results in an increase of microhardness (Fig. 7) which is consistent with the increase in elastic modulus also previously reported [9]. In fibres prepared at a higher pressure a better chain packing with an improvement in interfibrilar connectedness can be expected. As a result the resistance to slippage (proportional to $MH_{\perp}$), and the elastic properties of individual fibrils ($\sim MH_{\|}$) will be enhanced.

Previous observations [18] indicate the existence of a basic structural difference between the fibrous morphologies of the inner core (with a diameter $\sim 160\,\mu$m) and of the outer sheath of the strand (with a depth of ~ 170 to $200\,\mu$m). While the former consists of highly crystalline ribbons ~ 20 nm in diameter with a more prevalent extended chain structure at the centre of the extrudate, the latter is composed of ~ 300 nm fibres interconnected by a lamellar cross texture. Since the penetration depth of our indentations does not exceed 7–8 μm it is evident that all our microhardness data are releated to the mechanical properties of the more defective outer sheath. Thus the anisotropy increase with λ shown in Fig. 2 is consistent with the increasing number of the outer tie taut molecules bridging the lamellar cross texture in the fibre axis which account for the increasing elastic recovery with draw ratio along this direction.

In order to obtain some further information on the properties of the inner core, a few samples were cleaved along the fibre axis in the radial direction. Although the MH values at the inner core are ~ 15–20% lower than at the surface it is most revealing that ΔMH assumes values around 40% which are independent of λ (dotted line in Fig. 2). Thus the inner highly crystalline microfibrils exhibit the highest anisotropy irrespective of λ, presumably because these are mainly chain extended. At the fibre surface, on the contrary, ΔMH increases with λ because here the number of molecular connections gradually increases, tending in the limit for λ_{max} to reach the ΔMH value existing in the core. It seems, hence, that anisotropy measurements can detect some of the finer details of the microstructure of these highly oriented fibres.

The maximum attainable value of $MH_{\perp}$ (for $\lambda = 51$) (Fig. 5) – related to the plastic compression arising from slippage of fibrils and microfibrils perpendicularly to the fibre axis – is ~ 0.14 GPa. This value is approximately half the ideal ultimate compressive stress, assuming a value based on van der Waals forces for an ideally crystalline

solid, i.e. $S_\perp = \sigma/\partial l$, where σ is the energy per unit lateral surface area $\simeq 14.4\,\mathrm{mJ\,m^{-2}}$ [23] (force which must be applied per unit length to break the surface layer) and ∂l is the displacement between adjacent molecules and is assumed $\simeq 0.05$ nm. The numerous imperfections occurring in the solid due to the complex fibrillar structure parallel to the fibre axis are responsible for the lower experimental hardness value. Recent studies [24] obtained with isotropic PE indicate, in fact, that crystallinity deficiency and basal unit cell expansion markedly contribute to the depression of the microhardness value.

5. Conclusions

The following conclusions can be drawn from the above results

(1) The mechanical behaviour of extrusion drawn ultra-oriented PE strands can be defined in terms of a creep constant and a *MH* value at 0.1 min relating to the size of indentation under load.

(2) The *MH* at the surface of the strands is an increasing function of draw ratio, λ. The analytical character of the increase (whether exponential or a power function) depends on the extrusion temperature and pressure.

(3) The pure elastic release under the indenter is of the order of a 20% in the fibre direction and is negligible at right angles to it.

(4) The hardness anisotropy $\Delta MH = MH_{\parallel} - MH_{\perp}(\%)$ is a unique function of λ, following a law: $\Delta MH = a(\lambda - 1)^b$ and is independent of extrusion temperature and extrusion pressure. ΔMH is presumably correlated to the longitudinal elastic modulus and, hence, to the number of tie molecules.

(5) In the inner core of the strands ΔMH shows a constant value which is independent of λ and which coincides with the extrapolated value on the fibre surface for $\lambda_{max} = 51$.

(6) The value of the creep constant, K, is larger in the fibre direction than normal to it. The variation of K increases in the former and decreases in the latter direction with increasing temperature of extrusion. The dependence is consistent with the improvement of fibril to fibril cohesion and better chain packing arising at high extrusion temperatures.

Acknowledgement

The authors acknowledge the help of Mr Jaime Garcia Peña during the measurements of microhardness. Contributors from the University of Massachusetts would like to thank the Engineering Division of the National Science Foundation for supporting this study.

References

1. F. J. BALTÁ-CALLEJA, *Colloid and Polymer Sci.* **254** (1976) 258.
2. F. J. BALTÁ-CALLEJA and D. C. BASSETT, *J. Polymer Sci. Polymer Sym.* **58** (1977) 157.
3. F. J. BALTÁ-CALLEJA, W. T. MEAD and R. S. PORTER, *Polymer Eng. and Sci.*, in press.
4. A. PETERLIN, *J. Macromol. Sci. Phys.* **138** (1973) 83.
5. J. BOWMAN and M. BEVIS, *Colloid and Polymer Sci.* **255** (1977) 954.
6. K. NAKAYAMA and H. KANETSUNA, *J. Mater. Sci.* **12** (1977) 1477.
7. J. H. SOUTHERN and R. S. PORTER, *J. Macromol. Sci.* **4** (1970) 541.
8. A. E. ZACHARIADES, W. T. MEAD and R. S. PORTER, "Recent Developments in Ultraorientation of Polyethylene by Solid State Extrusion" edited by A. Ciferri and I. M. Ward (Applied Science Publishers, London, 1976).
9. R. S. PORTER, J. H. SOUTHERN and N. WEEKS, *Polymer Eng. and Sci.* **15** (1975) 213.
10. C. R. DESPER, J. H. SOUTHERN, R. D. ULRICH and R. S. PORTER, *J. Appl. Phys.* **41** (1970) 4284.
11. N. J. CAPIATI and R. S. PORTER, *J. Polymer Sci. Polymer Phys.* **13** (1975) 1177.
12. D. TABOR, "The Hardness of Metals" (Oxford University Press, Oxford, 1951).
13. K. MÜLLER, *Kunstoffe* **60** (1970) 265.
14. P. EYERER and G. LANG, *ibid.* **62** (1972) 322.
15. N. CAPIATI, S. KOJIMA, W. PERKINS and R. S. PORTER, *J. Mater. Sci.* **12** (1977) 334.
16. F. J. BALTÁ-CALLEJA and A. PETERLIN, *J. Macromol. Sci. Phys.* **B4** (1970) 519.
17. A. PETERLIN and F. J. BALTÁ-CALLEJA, *Kolloid Z.* **242** (1970) 1093.
18. R. G. CRYSTAL and J. H. SOUTHERN, *J. Polymer Sci.* **A2–9** (1971) 1641.
19. R. F. BISHOP, R. HILL and N. F. MOTT, *Proc. Phys. Soc.* **57** (1945) 148.
20. D. M. MARSH, *ibid.* **A279** (1964) 115.
21. K. L. JOHNSON, *J. Mech. Phys. Solids* **18** (1970) 115.
22. A. PETERLIN, *Kolloid Z.* **233** (1969) 858.
23. F. J. BALTÁ-CALLEJA and D. C. BASSETT (unpublished results).
24. J. MARTINEZ SALAZAR, Ph.D. Thesis, University of Madrid (1979).

Received 12 July and accepted 11 September 1979.